

Assessment of Left Ventricular Abnormal Twist in Repaired Tetralogy of Fallot Patients Using Phase-Contrast MRI

Meng-Chu Chang¹, Ming-Ting Wu², Marius Menza³, Mao-Yuan Su⁴, Hung-Chieh Huang², and Hsu-Hsia Peng⁵

¹Interdisciplinary Program of Nuclear Science, National Tsing Hua University, Hsinchu, Taiwan, ²Department of Radiology, Kaohsiung Veterans General Hospital,

Kaohsiung, Taiwan, ³Medical Physics, Department of Radiology, University Hospital Freiburg, Freiburg, Germany, ⁴Department of Medical Imaging, National Taiwan

University Hospital, Taipei, Taiwan, ⁵Department of Biomedical Engineering and Environmental Sciences, National Tsing Hua University, Hsinchu, Taiwan

Introduction: After the repaired surgery for patients with tetralogy of Fallot (rTOF), residual pulmonary regurgitation (PR) becomes the most problematic sequel, which leads to right ventricle (RV) volume overload and heart failure in the end (1). To prevent serious PR and the late cardiac failure, it is important to decide an appropriate timing for replacing the pulmonary valve. Geva et al. demonstrated a close linear correlation between the cardiac function, evaluated by cardiac MRI, of the RV and left ventricle (LV) in rTOF patients, suggesting the alteration in the geometry and function of the RV leads to LV dysfunction due to the shared myofibers (2). Previous studies demonstrated that LV rotation provided a feasible method for early detection of heart failure (3, 4). Menting et al. have evaluated LV rotation with speckle-tracking echocardiography (STE) in rTOF patients and concluded that over a quarter of patients had an abnormal apical rotation which correlated with decreased biventricular systolic function, suggesting that abnormal rotation may be an independent indicator for adverse ventricular function (5). Forementioned studies of LV rotation confined to global twist mechanics but were lack of discussing motion variation among myocardial segments. This study aims to evaluate regional circumferential velocity ($V\theta$) and the derived rotation in LV for rTOF.

Methods: The study recruited 16 rTOF patients (24.2 ± 4.4 y/o; male/female: 9/7) and 15 normal subjects (23.3 ± 2.4 y/o; male/female: 8/7) without any known cardiovascular diseases. The basic characteristics of cardiac function of two groups were shown in Table 1. All subjects were examined using 3.0 Tesla MR scanner (Trio with Tim or Skyra, Siemens, Erlangen, Germany). Prospective ECG-triggering (acquiring 90% of cardiac cycle) and navigator echo technique were performed to synchronize the cardiac and respiratory motion during free-breathing acquisitions, respectively. For the myocardial wall motion velocity, the imaging planes were placed on three short axis slices (Fig. 1a) and evaluated by three-directionally velocity encoded phase-contrast MRI with dark-blood technique: TR/TE = 26/4.2 ms, pixel size = 1.17×1.17 mm², slice thickness = 6 mm, flip angle = 7°, Venc in-plane = 15 cm/s and Venc through-plane = 25 cm/s. Post-processing was performed on a self-developed program. LV was divided into 16 segments (Fig. 1b). The temporal information was normalized to the period of end systolic time and shown as percentage of the systolic period (%ES). A 2D color plot of each subject was used to observe the time courses of $V\theta$ of 6 segments in the basal slice. To quantify the strength of twist function, an index of peak-to-peak (PTP) was defined to show the $V\theta$ difference between the counterclockwise (CCW) and clockwise (CW) peaks during the systolic phases (Fig. 2). $V\theta$ inconsistency, indicating dyssynchronous $V\theta$, is defined as the mean standard deviation (SD) of the systolic $V\theta$ among 6 segments in the basal slice. The angle of rotation was derived from velocity data to characterize cardiac twist function of each slice and defined as: $\text{Rotation} = \frac{V\theta(k) \times TR}{100} \times \frac{360}{2\pi \times R_{ave}}$, where k is the time frame; R_{ave} is the mean radius of LV. The net rotation angle was defined as the rotation difference between apical slice and basal slice. The indices of two groups were compared by two-tailed Student's t-test and $p < 0.05$ was considered statistical significance.

Results: Table 1 summarizes the basic characteristics of cardiac function of the study cohort. Patients with rTOF showed higher LVESVI (17.3 ± 6.0 vs. 14.4 ± 5.0 cm³/m², $p < 0.05$), LVEDV (97.8 ± 19.2 vs. 87.4 ± 13.5 cm³, $p < 0.05$), and LVEDVI (64.4 ± 11.1 vs. 54.2 ± 8.3 cm³/m², $p < 0.05$) than normals. In the 2D color plots, the normals generally showed a peak CCW $V\theta$ (-3.5 ± 0.2 cm/s) immediately after ECG R-wave, followed by a peak CW $V\theta$ (2.2 ± 0.1 cm/s) at 50 %ES (Fig.3). In contrast, rTOF patients displayed lower $V\theta$ either in the CCW peak (-1.3 ± 0.1) or in the CW peak (0.4 ± 0.1 cm/s). During early diastole (around 120 %ES ~ 140 %ES), rTOF patients exhibited dyssynchronized $V\theta$ among 6 segments of the basal slice, saying inconsistent diastolic peak CCW $V\theta$, in the color plots (Fig. 3). Figure 4 demonstrated that rTOF showed significant lower $V\theta$ PTP (5.5 ± 1.8 cm/s vs. 2.8 ± 1.3 cm/s, $p < 0.001$) and higher $V\theta$ inconsistency than normals (0.4 ± 0.1 cm/s vs. 0.5 ± 0.1 cm/s, $p < 0.01$). The typical time courses of rotation of two groups were shown in Fig. 5. The rTOF patients revealed reduced peak systolic rotation angles in basal, mid, and apical slices. At 40 %ES, normal group exhibited a mean peak systolic net rotation angle of $8.1 \pm 2.7^\circ$ and the peak was missing in rTOF patient ($3.9 \pm 1.7^\circ$ at 40 %ES) ($p < 0.001$).

Discussion & Conclusions: Sengupta et al described that twist leads to not only longitudinal, radial, and circumferential movements of the heart, but also contortion of the myocardium (6). Therefore, torsional mechanics can provide pathophysiological insight into the orientations of the myocardial fiber and myocardial contraction function. In this study, LV segmental $V\theta$ and rotation were assessed to present the twisting motion of the heart as well as its dyssynchrony for rTOF patients. A previous study has reported that rTOF patients presented abnormal twist mainly due to decreased apical rotation by using STE (5). In our work, decreased rotation angles were shown in three slices in rTOF (Fig. 5). In addition, a flat time course of net rotation evolution as well as delayed peak rotation can be observed in patients. Our recruited rTOF patients were with symptoms of cardiomyopathy, reflecting by increased LVESVI, LVEDV and LVESDI (Table 1). The recruited rTOF group showed comparable LVEF with normal (Table 1), suggesting that the cardiac function of patient group is not impaired yet. However, as shown in Fig. 4, the regional analysis showed lower $V\theta$ PTP and higher $V\theta$ inconsistency in rTOF patients, indicating our results can demonstrate dyssynchronous contraction in rTOF patients before deteriorated cardiac function. Leong et al. reported that myocardial fibrosis detected by late-gadolinium enhancement MRI is related to ventricular dyssynchrony in dilated cardiomyopathy patients, because the impaired myofibers tethered the shortening mechanics and redistribute the strain on myocardial fibers (7). Our finding about the higher $V\theta$ inconsistency shown in rTOF patients is likely associated with the myocardial fibrosis. In conclusion, $V\theta$ and the derived rotation angles were analyzed for rTOF patients and compared with age-matched normals. The lower $V\theta$ PTP and higher $V\theta$ inconsistency in rTOF patients suggested the abnormal dyssynchrony in rTOF patients before the cardiac function is impacted.

References: 1. T. Geva, *Semin Thorac Cardiovasc Surg*. 2006;9:11-22. 2. T. Geva, et al. *J Am Coll Cardiol*. 2004;43(6):1068-74. 3. M. Takeuchi, et al. *Eur Heart J*. 2007;28:2756-62. 4. J. Wang, et al. *Circulation*. 2007;116(22):2580-6. 5. M.E. Menting, et al. *Eur Heart J Cardiovasc Imaging*. 2014;15:566-74. 6. P.P. Sengupta, et al. *JACC Cardiovasc Imaging*. 2008;1:366-76. 7. D.P. Leong, et al. *Eur Heart J*. 2012;33:640-648.

Table 1. Basic characteristics of the study cohort.

	Normal (n=15)	rTOF (n=16)
Age (yrs)	23.3 ± 2.4	24.2 ± 4.4
Sex (male/female)	8/7	9/7
BSA (m ²)	1.6 ± 0.1	1.5 ± 0.2
LVESV (cm ³)	24.1 ± 6.2	26.2 ± 7.9
LVESVI (cm ³ /m ²)	14.4 ± 5.0	17.3 ± 6.0*
LVEDV (cm ³)	87.4 ± 13.5	97.8 ± 19.2*
LVEDVI (cm ³ /m ²)	54.2 ± 8.3	64.4 ± 11.1*
LVEF (%)	75.2 ± 5.1	73.6 ± 6.2

BSA: body surface area; LVESVI/LVEDVI: left ventricular end-systolic/end-diastolic volume index; LVEF: left ventricular ejection fraction. Data are presented as mean ± SD. * $p < 0.05$.

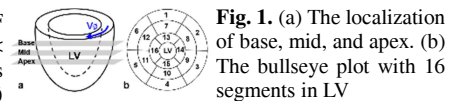


Fig. 1. (a) The localization of base, mid, and apex. (b) The bullseye plot with 16 segments in LV

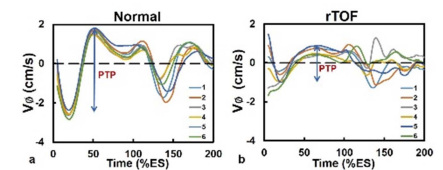


Fig. 2. The time course of $V\theta$ in basal slice of one normal (a) and one age-matched rTOF (b).

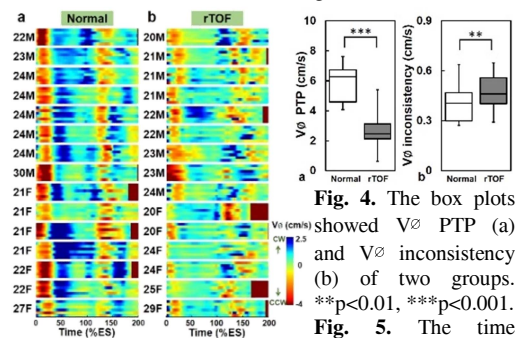


Fig. 4. The box plots showed $V\theta$ PTP (a) and $V\theta$ inconsistency (b) of two groups. *** $p < 0.01$, ** $p < 0.001$.

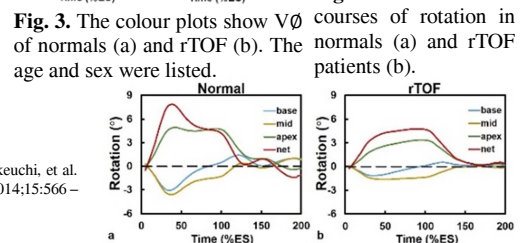


Fig. 3. The colour plots show $V\theta$ courses of rotation in normals (a) and rTOF (b). The age and sex were listed.

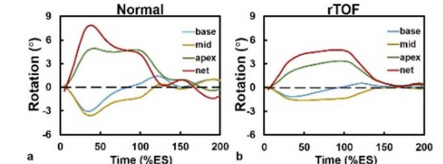


Fig. 5. The time courses of rotation in normals (a) and rTOF (b).